A Strength Analysis of a Hull Girder in a Rough Sea

Sa-Soo Kim *, Ku-Kyun Shin † and Sung-Wan Son ‡

(From T.S.N.A.K., Vol. 29, No. 4, 1992)

Abstract

A ship in waves is suffered from the various wave loads that comes from its motion throughout its life. Because these loads are dynamic, the analysis of a ship structure must be considered as the dynamic problem precisely. In the rationally-based design, the dynamic structural analysis is carried out using dynamic wave loads provided from the results of the ship motion calculation as a rigid body. This method is based on the linear theory assumed low wave height and small amplitude of motion. But at the rough sea condition, high wave height, compared with ship's depth, induce the large ship motion, so the ship section configuration under waterline is rapidly changed at each time. This results in a non-linear problem.

Considering above situation in this paper, a strength analysis method is introduced for the hull girder among waves considering non-linear hydrodynamic forces.

This paper evaluates the overall or primary level of the ship structural dynamic loading and dynamic response provided from the non-linear wave forces, and bottom flare impact forces by momentum slamming theory.For numerical calculation a ship is idealized as a hollow thin-walled box beam using thin walled beam theory and the finite element method is used.

This method applied to a 40,000 ton double hull tanker and attention is paid to the influence of the response of the ship's speed, wave length and wave height compared with the linear strip theory.

1. INTRODUCTION

When a ship proceeds through waves, not only it executes motions but also is deformed due to its flexibility. This deflection and distortion bring on various dynamic stresses in hull strength members. To predict dynamic behaviors of a ship among waves, it is practical that the hull girder is assumed as a non-uniform free-free beam. For the analysis of hull girder strength among waves, conventional techniques of seakeeping and structural analysis by the linear strip theory have achieved reasonable success. The basic idea of the method is to predict responses of a rigid ship against waves and to estimate wave exciting forces and

*Pusan National University
†Pusan National University; Presently at Agency for Defence Development
‡Pusan National University; Presently at Daewoo Shipbuilding & Heavy Machinery LTD

moments at each ship section. Integreating those static and dynamic pressures from after end of a ship to the fore end, hull girder strength is analyzed based on these wave exciting forces and moments.

Linear strip theory, however, in a restrict sense, has the fundamental limitation of small wave height and small responses of rigid ship because the hydrodynamic forces associated with hull (e.g. added masses, wave making damping forces) are calculated for the hull sections under the still water line.

In rough seas, configurations of transverse sections below the waterline are rapidly changed every moment due to large ship motion, and it is desirable not to ignore the nonlinear effect of hydrodynamic forces resulted from the nonlinearities in hull surface condition and free surface condition. As the case may be, a ship is exposed to a violent whipping vibration caused by slamming or green water effect. Especially, accidents that occurred in rough seas, which are probably due to slamming, have been reported [1]-[3].

The theoretical analysis of actual behaviors of a ship considering nonlinear hydrodynamic forces and slamming impact force have been attempted by many researchers. One of the earliest approaches to the specific problem of ship slamming from the view point of longitudinal hull girder strength was made by Ochi et al[4] and Kawakami, etc[5]. They evaluated the elastic response of a hull girder due to the slamming impact force at head seas. They calculated the ship motion as a rigid body and wave loads including impact force, which is estimated from relative velocity between hull bottom and wave surface. Fukasawa et al[6] and Kuroiwa et al[7] developed the theoretical evaluation of the motion and longitudinal strength of a ship in regular waves with large wave height taking account of nonlinearities of hydrodynamic forces on the bases of a concept which is similar to the strip theory. They formulated the equation of motion of a ship's hull as an elastic beam and the sectional added mass and wave making damping coefficient for vertical motion as a time-varying function. Their studies are only for the ship traveling in head seas, and therefore, it is difficult to apply their method to the estimation of the actual behavior of a ship in oblique waves, because of the nonlinearities of transverse and lateral hydrodynamic forces due to asymmetric section shape below instantaneous waterline resulted from large roll motion. Yoon[8] proposed more precise theoretical evaluation of the motion and wave loads of a ship in regular waves with large wave height taking account of nonlinearities of hydrodynamic forces. Yoon's study, however, has some limitation that hull bottom is not emerged, that is , slamming is not considered. This paper attempts more precise theoretical evaluation of the hull girder strength analysis in regular waves with large wave height considering hydrodynamic impact force using momentum slamming theorem and nonlinear effects due to the change of hull transverse submerged section, resulted from large ship motion. The elastic behavior of a ship is formulated by the thin-walled beam theory. The developed theory is applied to a 40,000 tons class double hull oil carrier preliminarily designed by Paik[9] and the ship motion and elastic behavior are calculated in head and bow quartering waves with changing wave height, wave length and ship speed. The computational results are compared with the results by the linear strip theory.

2. FORMULATION OF DYNAMIC BEHAVIOR OF A HULL GIRDER USING THIN-WALLED BEAM THEORY

2.1 Mathematical Model and Coordinate System

In Figure 1 a hull girder consisting complex structures is idealized as a thin-walled beam with varying section that have open section and closed sections located alternatively. The beam is divided into the elements which has the same properties within each element.

Element coordinates are taken as a right-hand coordinate system as shown in Figure 2

2.2 Finite element formulation

Assumptions are as follows for formulation:

1) The deflections are small in comparison with element dimensions.

2) Element material obeys Hook's law. par From Figure 3, it can be seen that for an arbitrary point p, displacement u in x-axis and u_s in tangential direction of yz plane are given by

$$u = -\theta(x)\omega(s) - \theta_z(x)y(s) + \theta_y(x)z(s) + u_x(x) \tag{1}$$

$$u_s = \theta(x)r(s) + u_y(x)\frac{\partial y(s)}{\partial s} + u_z(x)\frac{\partial Z(s)}{\partial s} \tag{2}$$

where u_x, u_y, u_z and θ_x, θ_y, θ_z are the displacement and rotation components in the x, y, z direction, respectively. $\theta(x)\omega(s)$ represents warping of the section and ω is the sectorial coordinate defined as

$$\omega(s) = \int_0^s \left(r - \frac{\psi}{t}\right) d\xi \tag{3}$$

where ψ is torsional function and t is thickness.

Therefore, the strain-displacement relations are as follows:

$$\epsilon_x = -\theta_\omega{}' - \theta_z{}' y - \theta_y{}' z - u_x{}' \tag{4}$$

$$\begin{aligned}\gamma_{xs} &= \theta_x{}' r + u_y{}' \frac{\partial y}{\partial s} + u_z{}' \frac{\partial z}{\partial s} + \theta \frac{\partial \omega}{\partial s} + \theta_z \frac{\partial y}{\partial s} \\ &= \frac{\psi}{t}\theta + (\theta_x{}' - \theta)r + (u_y{}' - \theta_z)\frac{\partial y}{\partial s} + (u_z{}' + \theta_y)\frac{\partial z}{\partial s}\end{aligned} \tag{5}$$

The prime indicates differentiation with respect to x. The kinetic energy E_e, the strain energy U_e and the work done by external forces W_e in an element are

$$E_e = \frac{1}{2}\rho_s \int_V (\dot{u}^2 + \dot{u}_s^2) dV \tag{6}$$

$$U_e = \frac{1}{2}\int_V (E\epsilon_x{}^2 + G\gamma_{xs}{}^2) dV \tag{7}$$

$$W_e = \int_V (f_x u + f_s u_s) dV \tag{8}$$

where,

ρ_s : density of element
E : Young's modulus
G : shear modulus
V : volume
f_x : x – directional external force per unit volume
f_s : tangential direction external force in yz plane

Let's express displacement $\{u(x,t)\}^T = \{u_x u_y u_z \theta_x \theta_y \theta_z\}$ in terms of the components of displacement at the nodes using interpolation functions $[N]$.

$$\{u(x,t)\} = [N]\{q(t)\} \tag{9}$$

where,

$$\{q(t)\} = \{u_{x1}, u_{y1}, u_{z1}, \theta_{x1}, \theta_{y1}, \theta_{z1}, u_{x2}, u_{y2}, u_{z2}, \theta_{x2}, \theta_{y2}, \theta_{z2}\}$$

Therefore, substituting equations (1) ~ (5) and (9) into equations (6), (7), (8) and applying Hamilton's principle

$$\delta \int_{t_1}^{t_2} (E - U + W) dt = 0 \tag{10}$$

E : total kinetic energy of system
U : total strain energy of system
W : total work done by external force of system

gives the discretized equation of motion

$$[M]\{\ddot{q}\} + [K]\{q\} = \{F\} \tag{11}$$

where $[M]$ and $[K]$ is the mass and stiffness matrix of a hull girder, respectively.

In order to consider structural damping effect of the hull girder, viscous damping is assumed. The most common form of damping, so-called Rayleigh type damping, is given by

$$[C] = \alpha[M] + \beta[K]$$

The two constants α and β can be determined by the property of material and shape of elements. Therefore, the final motion of equation considered damping can be derived as follows:

$$[M]\{\ddot{q}\} + [C]\{\dot{q}\} + [K]\{q\} = \{F(t)\} \tag{12}$$

3. EVALUATION OF NONLINEAR HYDRODYNAMIC FORCES

Nonlinear hydrodynamic forces due to wave is evaluated by strip method, but it is assumed that wave height is relatively larger than the draft and the configuration of cross sections under the instantaneous water line is changed according to the ship motion. The slamming impact force which occurs when ship bottom reenters into the water after bottom emergence is evaluated by the momentum slamming theory. In oblique wave, coupling effects of transverse-lateral hydrodynamic forces which are caused by large unsymmetric transverse sections due to large roll motion are considered.

3.1 Coordinate System

The rectangular coordinate system is introduced as shown in Figure 4. Let a ship travel with constant speed U in the direction of x in regular wave with wavelength λ and wave amplitude α (= a half of wave height). The coordinate system ($o' - x'y'z'$) originated at

midship on the still water surface is moved with the ship and the coordinate system (O-XYZ) originated on the still water surface is spatially fixed.

3.2 Nonlinear Hydrodynamic Forces

The forces applied to ship transverse sections can be represented by the sum of hydrodynamic forces and hydrostatic forces. But the forces in x direction is neglected in this formulation.

Therefore,

$$\begin{aligned} \delta F_y &= \delta F_{Hy} + \delta F_{Sy} \\ \delta F_z &= \delta F_{Hz} + \delta F_{Sz} \\ \delta M_x &= \delta M_{Hx} + \delta M_{Sx} \end{aligned} \tag{13}$$

where subscripts H and S denote the hydrodynamic force and the hydrostatic force, respectively.

3.2.1 Hydrodynamic Forces

Based on the momentum theory, the hydrodynamic forces and moments applied to the section at $x = x$ can be expressed as follows:

$$\begin{aligned} \delta F_{Hy} = & -\frac{D}{Dt}\left[m_{SS}\frac{D\bar{u}_y}{Dt} + m_{SH}\frac{D\bar{u}_z}{Dt} + m_{SR}\frac{D\bar{\theta}_x}{Dt}\right] \\ & \left[N_{SS}\frac{D\bar{u}_y}{Dt} + N_{SH}\frac{D\bar{u}_z}{Dt} + N_{SR}\frac{D\bar{\theta}_x}{Dt}\right] \end{aligned} \tag{14}$$

$$\begin{aligned} \delta F_{Hz} = & -\frac{D}{Dt}\left[m_{HS}\frac{D\bar{u}_y}{Dt} + m_{HH}\frac{D\bar{u}_z}{Dt} + m_{HR}\frac{D\bar{\theta}_x}{Dt}\right] \\ & \left[N_{HS}\frac{D\bar{u}_y}{Dt} + N_{HH}\frac{D\bar{u}_z}{Dt} + N_{HR}\frac{D\bar{\theta}_x}{Dt}\right] \end{aligned} \tag{15}$$

$$\begin{aligned} \delta M_{Hx} = & -\frac{D}{Dt}\left[m_{RS}\frac{D\bar{u}_y}{Dt} + m_{RH}\frac{D\bar{u}_z}{Dt} + m_{RR}\frac{D\bar{\theta}_x}{Dt}\right] \\ & \left[N_{RS}\frac{D\bar{u}_y}{Dt} + N_{RH}\frac{D\bar{u}_z}{Dt} + N_{RR}\frac{D\bar{\theta}_x}{Dt}\right] \end{aligned} \tag{16}$$

where H, S and R denotes the heave, sway and roll motion and m_{ij}, N_{ij} is the time-varying sectional added mass and wave damping coefficient of the ith-mode motion due to the jth $-$ mode motion.

Differential operator D/Dt is defined as

$$\frac{D}{Dt} = \frac{\partial}{\partial t} - U\frac{\partial}{\partial x}$$

$\bar{u}_x$, $\bar{u}_z$ and $\bar{\theta}_x$ is relative transverse, lateral and rotational displacement of an arbitrary point

in the section.

3.2.2 Hydrostatic Forces

The hydrostatic force can be represented by the force resulted from the pressure of incident wave including the change of hydrostatic pressure. As shown in Figure 5, if the transverse section configuration below instantaneous water line at any time is determined, then the hydrostatic forces are evaluated by integrating internal pressure of incident wave along the girth of the submerged section.

The pressure can be expressed by the generalized Bernoulli's equation as follows:

$$\begin{aligned} p = \; & \rho g(z' - \zeta) - \rho \left[\frac{\partial \phi_w}{\partial t} - \left[\frac{\partial \phi_w}{\partial t} \right]_{z=\zeta} \right] \\ & \frac{1}{2}\rho \left([\nabla \phi_w]^2 - [\nabla \phi_w]^2{}_{z=\zeta} \right) \end{aligned} \tag{17}$$

In equation (17), wave surface ζ is

$$\zeta = a\cos(k\cos\chi x' - k\sin\chi y' - \omega_e t) \tag{18}$$

where, k is wave number, ω_n is wave encounter frequency, a is amplitude of wave and χ is incident wave angle. Incident wave potential ϕ_w is

$$\phi_w = -\frac{ga}{\omega}\exp[-kz'](k\cos\chi x' - k\sin\chi y' - \omega_e t)$$

where, g is acceleration of gravity and ω is incident wave frequency. Therefore equation (17) can lead

$$\begin{aligned} p = \; & \rho g(z' - \zeta) - \rho g(\exp(-kz') - \exp(-\zeta)) \\ & \times \cos(k\cos\chi x' - k\sin\chi y' - \omega_e t) \\ & \frac{1}{2}\rho a^2\omega^2((\exp(-2kz') - \exp(-2k\zeta)) \end{aligned} \tag{19}$$

Using equation (19), hydrostatic force and moments in x', y' and z' direction can be expressed by

$$\delta F_{sy} = \rho \int_A^B p dz \tag{20}$$

$$\delta F_{sz} = W + \int_A^B (-p) dy' \tag{21}$$

$$\delta M_{sx} = W(Z_s' - Z_g')\sin\theta + \int_A^B p(-y dy' - z dz')$$

Where W is weight of hull girder per unit length, and A, B is instantaneous water line at starboard and port.

3.2.3 Force Vector Due to Wave

Let nonlinear hydrodynamic forces apply to a thin-walled beam element with length l as distributed force. Then force vector can be obtained by integrating along element length l as

follows:

$$\begin{Bmatrix} F_x \\ F_y \\ F_z \\ M_x \\ M_y \\ M_z \end{Bmatrix} = \int_0^1 \begin{Bmatrix} 0 \\ \delta F_{Hy} + \delta F_{sy} \\ \delta F_{Hz} + \delta F_{sz} \\ \delta F_{Hx} + \delta F_{sx} \\ 0 \\ 0 \\ 0 \end{Bmatrix} dx$$

$$\begin{aligned} &= [B_1]\int_0^1 \{\ddot{u}\}dx + [B_2]\int_0^1 \{\dot{u}\}dx - 2U[B_1]\int_0^1 \{\dot{u}'\}dx \\ &\quad + U[B_2]\int_0^1 \{u'\}dx + U^2[B_1]\int_0^1 \{u''\}dx \\ &\quad + \int_0^1 [B_3]\{w_{f1}\}dx - \int_0^1 [B_4]\{w_{f2}\}dx \\ &\quad + \int_0^1 \{F_{s1}\}dx + \int_0^1 [F_{s2}]\{u\}dx \end{aligned} \tag{22}$$

where

$$[B_1] = \begin{bmatrix} 0 & 0 & 0 & 0 & 0 & 0 & 0 \\ 0 & m_{SS} & m_{SH} & -z_S m_{SS} + m_{SR} & 0 & 0 & 0 \\ 0 & m_{HS} & m_{HH} & -z_S m_{HS} + m_{SR} & 0 & 0 & 0 \\ 0 & m_{RS} & m_{RH} & -z_S m_{RS} + m_{RR} & 0 & 0 & 0 \\ 0 & 0 & 0 & 0 & 0 & 0 & 0 \\ 0 & 0 & 0 & 0 & 0 & 0 & 0 \\ 0 & 0 & 0 & 0 & 0 & 0 & 0 \end{bmatrix}$$

$$[B_2] = \begin{bmatrix} 0 & 0 & 0 & 0 & 0 & 0 & 0 \\ 0 & C_{SS} & C_{SH} & -z_S C_{SS} + C_{SR} & 0 & 0 & 0 \\ 0 & C_{HS} & C_{HH} & -z_S C_{HS} + C_{HR} & 0 & 0 & 0 \\ 0 & C_{RS} & C_{RH} & -z_S C_{RS} + C_{RR} & 0 & 0 & 0 \\ 0 & 0 & 0 & 0 & 0 & 0 & 0 \\ 0 & 0 & 0 & 0 & 0 & 0 & 0 \\ 0 & 0 & 0 & 0 & 0 & 0 & 0 \end{bmatrix}$$

$$[B_3] = \begin{bmatrix} 0 & 0 & 0 & 0 & 0 & 0 & 0 \\ 0 & C_{SS} & C_{SH} & C_{RS} & 0 & 0 & 0 \\ 0 & C_{HS} & C_{HH} & C_{HR} & 0 & 0 & 0 \\ 0 & C_{RS} & C_{RH} & C_{RS} & 0 & 0 & 0 \\ 0 & 0 & 0 & 0 & 0 & 0 & 0 \\ 0 & 0 & 0 & 0 & 0 & 0 & 0 \\ 0 & 0 & 0 & 0 & 0 & 0 & 0 \end{bmatrix}$$

$$[B_4] = \begin{bmatrix} 0 & 0 & 0 & 0 & 0 & 0 & 0 \\ 0 & m_{SS} & m_{HS} & m_{RS} & 0 & 0 & 0 \\ 0 & m_{SH} & m_{HH} & m_{RH} & 0 & 0 & 0 \\ 0 & m_{SR} & m_{HR} & m_{RR} & 0 & 0 & 0 \\ 0 & 0 & 0 & 0 & 0 & 0 & 0 \\ 0 & 0 & 0 & 0 & 0 & 0 & 0 \\ 0 & 0 & 0 & 0 & 0 & 0 & 0 \end{bmatrix}$$

$$\{w_{f1}\} = \begin{Bmatrix} 0 \\ \partial\omega \exp[-kd_1]\{\cos Q_b - \cos Q_a\}/k \sin x(y_{b'} - y_{a'}) \\ -\partial\omega \exp[-kd_2]\{\sin Q_b - \sin Q_a\}/k(y_{b'} - y_{a'}) \\ \partial\omega \exp[-kd_2]\{\sin Q_b - \sin Q_a\}/(y_{b'} - y_{a'}) \\ 0 \\ 0 \\ 0 \end{Bmatrix}$$

$$\{w_{f2}\} = \begin{Bmatrix} 0 \\ \partial\omega^2 \exp[-kd_1]\{\sin Q_b - \sin Q_a\}/k \sin x(y_{b'} - y_{a'}) \\ \partial\omega^2 \exp[-kd_2]\{\cos Q_b - \cos Q_a\}/k(y_{b'} - y_{a'}) \\ -\partial\omega^2 \exp[-kd_2]\{\cos Q_b - \cos Q_a\}/(y_{b'} - y_{a'}) \\ 0 \\ 0 \\ 0 \\ 0 \end{Bmatrix}$$

$$\{F_{s1}\} = \begin{Bmatrix} \rho g \int_a^b (z' - a((1 + \exp(-kz') - \exp(-k\zeta)) \\ \cos(k \cos \chi x' - k \sin \chi y' - \omega_e t))dz' \\ -1/2\rho g a^2 \omega^2 \int_a^b ((\exp(-2kz') - \exp(-2k\zeta))dz' \\ \rho g A_{so} + \rho g \int_a^b -z' + a((1 + \exp(-2kz') \\ - \exp(-k\zeta)) \cos(k \cos \chi x' - k \sin \chi y' - \omega_e t))dy' \\ +1/2\rho a^2 \omega^2 \int_a^b ((\exp(-2kz') - \exp(-2k\zeta))dy' \\ \rho g \int_a^b (-z' - a((1 + \exp(-kz') - \exp(-k\zeta)) \\ \cos(k \cos \chi x' - k \sin \chi y' - \omega_e t))(y'dy' + z'dz') \\ +1/2\rho a^2 \omega^2 \int_a^b (\exp(-2kz') - \exp(-2k\zeta))(y'dy' + z'dz') \\ 0 \\ 0 \\ 0 \end{Bmatrix}$$

$$[F_{s2}] = \begin{bmatrix} 0 & 0 & 0 & 0 & 0 & 0 & 0 \\ 0 & 0 & 0 & 0 & 0 & 0 & 0 \\ 0 & 0 & 0 & \omega(z_s - z_g) & 0 & 0 & 0 \\ 0 & 0 & 0 & 0 & 0 & 0 & 0 \\ 0 & 0 & 0 & 0 & 0 & 0 & 0 \\ 0 & 0 & 0 & 0 & 0 & 0 & 0 \\ 0 & 0 & 0 & 0 & 0 & 0 & 0 \end{bmatrix}$$

$$
\begin{aligned}
C_{ij} &= \dot{m}_{ij} - Um_{ij}' + N_{ij}(i,j = S,R,H) \\
Q_a &= k\cos\chi x' - k\sin\chi y_a' - \omega_e t \\
Q_b &= k\cos\chi x' - k\sin\chi y_b' - \omega_e t \\
d_1, d_2 &: \text{representative draft of section}
\end{aligned}
$$

Representing the force vector of equation(22) as a nodal force vector using relation of equation (9), the nodal force vector in equation (12) can be expressed as follows:

$$
\begin{aligned}
\{F(t)\} &= \left[\int_0^1 [N]^T[B_1][N]dx\right]\{\ddot{q}(t)\} \\
&\quad + \left[\int_0^1 [N]^T[B_2][N]dx - 2U\int_0^1 [N]^T[B_1]d/dx[N]dx\right]\{\dot{q}(t)\} \\
&\quad + \left[-U\int_0^1 [N]^T[B_2]d/dx[N]dx + U^2\int_0^1 [N]^T[B_1]d^2/dx^2[N]dx\right. \\
&\quad \left. + \int_0^1 [N]^T[F_{s2}][N]dx\right]\{q(t)\} \\
&\quad + \int_0^1 \left[-[N]^T[B_3]\{w_{f1}\} - [N]^T[B_4]\{w_{f2}\} + [N]^T\{F_{s1}\}\right]dx \\
&= [M_f]\{\ddot{q}(t)\} + [C_f]\{dotq(t)\} + [K_f]\{q(t)\} + \{F_t\} \qquad (23)
\end{aligned}
$$

4. ESTIMATION OF RIGID BODY MOTION AND VIBRATION RESPONSE

4.1 Equation of Motion

Using the mass matrix, damping matrix and stiffness matrix as mentioned in chapter 2 and 3, the equation of motion for entire system can be expressed as follows:

$$
\begin{aligned}
&[M_G]\{\ddot{Q}(t)\} + [C_G]\{\dot{Q}(t)\} + [K_G]\{Q(t)\} \\
&= [M_{fG}]\{\ddot{Q}(t)\} + [C_{fG}]\{\dot{Q}(t)\} + [K_{fG}]\{Q(t)\} + \{F_{fG}\} \qquad (24)
\end{aligned}
$$

where, let assume that displacement vector $Q(t)$ can be divided into a rigid body displacement Q_r and an elastic displacement Q_e. For simplicity, added mass for the elastic vibrating modes is used that for hull section in still water at infinite frequency, and its 3 dimensional correction factor is taken the value of second mode of vertical, horizontal and torsional vibration respectively. The wave damping and hydrostatic restoring force for elastic vibration are neglected. Based on the above assumption, the right side term of equation (24) can be written as follows:

right side term =

$$
[M_{fg}]\omega_e\{\ddot{Q}_r\} + [C_{fg}]\omega_e\{\dot{Q}_r\} + [K_{fg}]\omega_e\{Q_r\} + \{F_G\} + [M_{fg}]_\infty\{Q_e\} \qquad (25)
$$

where, ω_e is encountering frequency, and ∞ denotes infinite frequency. $[M_{fg\infty}]$ is the hydrodynamic force matrix which is called added mass for elastic vibration. Because it is assumed time-invariant quantity, this matrix can be moved to the left.

$$
\begin{aligned}
&\{[M_G] + [M_{fg}]_\infty\}\{\ddot{Q}_e(t)\} + [C_G]\{\dot{Q}_e(t)\} + [K_G]\{Q_e(t)\} \\
&= [M_{fg}]\omega_e\{\ddot{Q}_r(t)\} + [C_{fG}]\omega_e\{\dot{Q}_r(t)\} + [K_{fg}]\omega_e\{Q_r\} + \{F_{fg}\} \qquad (26)
\end{aligned}
$$

Since the coefficient matrices of the left in equation (26) are independent of the time, the modulus can be obtained by solving eigenvalue problems using equation (26).

Let the response of forced vibration expressed as a linear combination of the eigen vectors with rigid body modes and elastic modes. Then the displacement vector $Q(t)$ can be written in the form

$$\begin{aligned} \{Q\} &= [P_r, P_e]\begin{bmatrix} I_r \\ I_e \end{bmatrix} \\ &= [P_r]\{I_r\} + [P_e]\{I_e\} \end{aligned} \tag{27}$$

where

$[P_r]$: rigid body mode
$[P_e]$: elastic mode
$\{I_r\}$: weighting function of rigid body mode
$\{I_e\}$: weighting function of elastic mode

Since the rigid body displacements do not affect the elastic displacements and structural damping forces, following relations can be obtained.

$$[P_r]^T[K_G] = 0$$
$$[P_e]^T[K_G] = 0$$

Using the orthogonality condition between modes and the above relations, equation (26) can be divided into following two equations (28),(29) according to premultiplying equation (26) by $[P_r]^T$ and $[P_e]^T$, respectively.

$$([M_r] - [m_r])\{\ddot{I}_r\} + (-[C_r])\{\dot{I}_r\} + (-[K_r])\{I_r\} = \{f_r\} \tag{28}$$

$$\begin{aligned} &([M_e])\{\ddot{I}_e\} + (-[C_e])\{\dot{I}_e\} + (-[K_e])\{I_e\} \\ &= ([m_e])\{\ddot{I}_r\} + (-[C_e])\{\dot{I}_r\} + (-[K_e])\{I_r\} + \{f_e\} \end{aligned} \tag{29}$$

where,

$$\begin{aligned} [M_r] &= [P_r]^T[M_G][P_r] \quad [m_r] = [P_r]^T[M_{fG}]\omega_e[P_r] \\ [C_r] &= [P_r]^T[C_{fG}]\omega_e[P_r] \quad [K_r] = [P_r]^T[K_{fG}]\omega_e[P_r] \\ [f_r] &= [P_r]^T[F_{fG}] \\ [M_e] &= [P_e]^T[M_{fG}]_\infty[P_e] + [P_e]^T[M_G][P_e] \\ [C_e] &= [P_e]^T[C_G][P_e] \quad [K_e] = [P_e]^T[K_G][P_e] \\ [m_e] &= [P_e]^T[M_{fG}]\omega_e[P_r] \quad [C_e] = [P_e]^T[C_{fG}]\omega_e[P_r] \\ [K_e] &= [P_e]^T[K_{fG}]\omega_e[P_r] \quad [f_e] = [P_e]^T[F_{fG}] \end{aligned}$$

Since the coefficient matrices are dependent of time, the equations are nonlinear. To solve these equations, Newmark-β method, one of the time stepping analysis methods, is used.

4.2 Numerical Calculation

The element of matrices in equation (28) and (29), the added mass and the wave damping coefficient, are calculated by the close-fit method proposed by Frank[12]. The hydrodynamic

impact force is estimated by the change of added mass with the time. Ship side shell is assumed to be extend infinitely because the green water effect is not considered. The rigid body responses at any time are calculated by solving equation (28) and the elastic responses at that time are calculated by substituting rigid body responses into equation (29).

4.3 Shearing Force, Bending Moment and Torsional Moment

To calculate shearing force, bending moment and torsional moment, we used the equation as follows:

$$\begin{aligned} \bar{M}_h &= -EI_z\ddot{u}_y \\ \bar{F}_h &= -EI_z\ddot{u}_y \\ \bar{M}_v &= -EI_y\ddot{u}_z \\ \bar{F}_v &= -EI_y\ddot{u}_z \\ \bar{M}_t &= GJ\dot{\theta}_x + EI_w\ddot{\theta}_x \end{aligned}$$

where,

$\bar{M}_h$: Horizontal bending moment
$\bar{F}_h$: Horizontal shearing force
$\bar{M}_v$: Vertical bending moment
$\bar{F}_v$: Vertical shearin force
$\bar{M}_t$: Torsional moment
EI_y : Horizontal stiffness
EI_z : Vertical stiffness
GJ : Torsional stiffness of saint – venant
EI_w : Warping stiffness

5. NUMERICAL CALCULATION AND CONSIDERATION

5.1 Verification of the Proposed Dynamic Strength Analysis Method

To verify the analysis theory developed in this study, we selected the model ship which Fukasawa has experimented [26] and compared the numerical results of this analysis with those of the model experiment. The principal dimensions of the model ship are listed in Table 1. Numerical calculations were carried out under the condition that Froude Number(F_n) is 0.154, incident wave angle(χ) 157.5°, wave length(λ/L) 1.2, ship length/wave height(L/H_w) 30. The results are compared with the measured strain value from the strain gauge attached on the main deck of the midship section as shown in Figure 6. From that comparison, we could conclude that the theoretical analysis method presented here gives good agreements with the estimation results and is illustrated in Figure 7.

5.2 The Investigation of the Response Characteristics of a 40,000 Ton Double Hull Tanker by Changing the Wave Height, Wave Length and Wave Speed.

To analyze the effect of the hull vibration response and wave load characteristics by changing the wave height, wave length and wave speed, we selected a 40,000 ton double-skin tanker.

And all of this calculation results are compared with calculation results by linear strip theory, changing the wave length $\lambda/L = 1.0, 1.5, 2.0$ and the wave height $L/H_w = 25, 20, 15$ and speed $F_n = 0.1, 0.15, 0.2$ in head wave($\chi = 180^o$) and oblique wave condition. The wave load is nondimensionalized as follows:

$$\begin{aligned} F_v &= \bar{F}_v/\rho g L b a \\ M_v &= \bar{M}_v/\rho g L^2 b a \\ F_h &= \bar{F}_h/\rho g L b a \\ M_h &= \bar{M}_h/\rho g L^2 b a \\ M_t &= \bar{M}_t/\rho g L^2 b a \end{aligned} \tag{30}$$

where,

ρ : density
g : gravitational acceleration
L : ship length
b : ship width
a : wave amplitude

5.2.1 Ship for Numerical Calculation (Test Ship)

The principal dimensions of the test ship is listed in Table 2 and the general arrangement plan is shown in Figure 8 and the body plan and the configuration of midship section and shearing force distribution curve, bending moment distribution curve in the still water condition of ship are shown in Figure 9, Figure 10, and Figure 11 respectively. As shown in Figure 11, by assuming the load condition to be 2/3 of the full load condition, it can be known that there arises about 7,000 ton-m still water hogging moment in the vicinity of the midship section by alternatively distributing cargoes in cargo area one by one.

5.2.2 The Behavior in Head Wave ($x = 180^o$)

(1) rigid body response

In Figure 12 and Figure 13, the compared results of the rigid body response in head wave ($x = 180^o$) -heave and pitch- with the result of the linear strip theory is shown. As shown in Figure 12, for the heaving motion, the non-linear calculation gives larger values than those in linear calculation at the position $\lambda/L = 1.0$ for $F_n = 0.1$ and $\lambda/L = 1.5$ for $F_n = 0.15, 0.2$.

The excessive changing rate of the draft of the hull section, in other words the exposure of the bow and bottom in the air, has seemed to increase the non-linear fluid force effect. In Figure 13, by contraries in heave motion, the non-linear calculation results for pitch motion are lower than those of linear theory and this difference increases at the high wave height.

(2) wave load

1) The distribution of wave load along the ship length

In Figure 14, and Figure 15, the result of the wave load distribution along the ship hull at the smallest wave height ($L/H_w = 25$) and $\lambda/L = 1.0$ in head wave($\chi = 180^o$) is compared with that of linear strip theory. As shown in Figure 14, the maximum value of vertical shear force is close to that of linear calculation but there are some differences in distribution shape along the ship length. This means, as comparing with the linear calculation, that the position

which the maximum vertical shear force occurred was shifted forward at the bow part and afterward at the stern part. And this shift grows as the ship speed increases.

This means that if the draft of bow and stern rises up to the bow and flare and deck led to changing abruptly the wet section shape, it increases the non-linearity of the fluid force. Also, as shown in Figure 15, the position of the maximum bending moment is shifted forward to the bow compared to the position of linear calculation.

2) Maximum wave load

The maximum wave load calculation results of non-linear theory comparing to those of linear theory are shown in Figure 16 and Figure 17.

Now, for the case that the bottom is emerged and is acted by the fluid impact, we can understand, that the maximum load of non-linear calculation is higher than that of the linear theory and hogging moment is larger than the sagging.

The reason is that due to the emergence of the extensive part of the bow in the air, the weight of bow brings out the hogging moment. But, when the bottom exposure is not so severe, the calculation result of both linear and non-linear approached becomes similar and the dimensionless vertical wave load increases as the wave height and ship speed increase.

3) The time history of vertical bending moment

To estimate the characteristics of the wave load with time, the position of the maximum bending moment distribution and its time variance along the ship length with the varying ship speed is shown in Figure 18. As shown in Figure 18(a), the bottom impact arises during the period that the bottom is changing from hogging to sagging condition and in Figure 18(b), there are some complex shapes for the distribution of the vertical bending moment along the ship length for the case of bottom exposure and the bottom impact. But in that case, it reveals that the maximum bending moment gives two-node vibration pattern mainly and the three-node and the higher node vibrations are relatively small in magnitude and the speed of damping is higher.

5.2.3 The Behavior in Oblique Wave ($\chi = 120^o$)

(1) Rigid body response

In Figure 19 $\sim$ Figure 23, the results of the rigid body response in an oblique wave($\chi = 120^o$) -heave, pitch, sway, yaw,and roll motion- are compared with the result of the linear strip theory. The heave and pitch motion show the similar pattern in head wave and give little difference in nonlinear and linear calculation results.

For the nondimensional response of the yaw motion, the linear calculation is higher than that of the non-linear one and is getting higher with the increase of wave height. But for the sway and roll motion, as for the linear calculation, the effect of non-linearity caused by draft change is much more sensitive than for other motions.

For the roll motion, we thinks that the difference between the linear and non-linear calculation results from calculation method. Especially linear theory, it is assumed that the restoring moment is proportional to the hull inclinement, but in non-linear theory, the restoring moment is evaluated by integration over instantaneous transverse sectional area below water line.

(2) Wave load

1) Distribution of wave load along the ship length

In Figure 24 $\sim$ Figure 28, the distributions of wave load along the ship at the smallest wave height ($L/H_w = 25$) and $\lambda/L = 1.0$ in oblique wave($\chi = 120^o$) are shown.

For vertical shear force and bending moment, magnitude and distribution shape have similar pattern in linear and non-linear calculation. But,it is similar to the result in head sea that the position which has maximum value is moved to afterbody.

For horizontal shear force and bending moment, distribution in linear and nonlinear calculation have some differences, especially these are some differences in + and −.

We can say that the configuration of underwater section is rapidly changing and increment of the relative position between the ship and wave is larger in starboard than in port for the effect of incident wave angle, ship speed and ship motion.

For torsional moment, we know that the difference of distribution shape is large. The reason of this is that in horizontal shear force and horizontal bending moment, the linear computation evaluates wave load by integrating to the direction of ship length, on the contrary in this paper, we evaluate torsional moment from the rotational displacement curve. Thus we can say that the difference between these methods of calculations affected too.

2) Maximum wave load

In Figure 29 $\sim$ 33, the magnitudes of the maximum wave load are shown. When bottom emerges, the difference between linear and nonlinear calculation is large in vertical shear force and vertical bending moment.

But the effect of slamming is much smaller than in headwave because the relative velocity between the ship and water surface is small due to the small heave and pitching motion.

And the hogging moment is larger than the sagging moment as similar as in headwave. And the same trends appear when there is no emerge of the ship bottom.

The nondimensional wave load of horizontal shearing force and torsional moment increases at large wave height and short wave length compared with linear calculation.

The ship speed does not affect largely on vertical wave loads. But in small wave height, we think, the difference between linear calculation and nonlinear calculation will be resulted from the difference of the rigid body response(refer to Figure 21,23).

6. CONCLUSION

A theoretical evaluation of the hull girder dynamic behavior, in regular waves of large wave height, considering hydrodynamic impact force due to slamming and nonlinearities by ship motions is attempted. And numerical calculation is carried out for a 40,000 ton oil tanker by varying parameters such as wave height, wave length and ship's speed in head wave ($\chi = 180^o$) and oblique wave ($\chi = 120^o$). The results of this study are summarized as follows:

1) The theoretical evaluation attempted in this study is verified its usefulness by comparing with Fukasawa's experimental results.

2) Since the rigid body response and wave loads do not greatly differ from the results of linear calculation at no bottom emergence condition, the linear strip method, in practical, is reasonable.

3) Nonlinear hydrodynamic forces and elastic response charac- teristics have to be considered when the ship bottom emerges and slamming occurs because of the increase of nonlinear effects.

4) In this study, numerical calculations are carried out only in head wave($\chi = 180^o$) and oblique wave($\chi = 120^o$), so it is necessary to analyze in beam wave and following wave.

Especially, we think that research on nonlinear effect for various types of ship has to be continued.

References

[1] Masuo Kawakami,Hiromitsu Muramoto, "On the Damage of Bottom of Small Ships due to Slamming," *The Society of Naval Architects of West Japan*, Vol. 33, 1966

[2] Y.Yamamoto, M.Fujino, H.Ohtsubo, T.Fukazawa, G.Aoki, H.Ikeda, A.Kumano, "Analysis of Disastrous Structural Damage of a Bulk Carrier," PRADS 83, 1983

[3] Report of Investigation on the Onomichimaru's Disaster.Breau of Ship, Ministry of Transportation of Japan, 1981

[4] M.K.Ochi and L.E.Motter, "Prediction of Slamming Characteristics and Hull Response for Ship Design," *Trans. SNAME*, Vol. 81, 1973

[5] Masuo Kawakami, Kazuo Kobayashi, "On Whipping Vibration of Ship Body due to Slamming Impact," *The Society of Naval Architects of West Japan*, Vol. 50, 1975

[6] Y. Yamamoto, M. Fujino, T. Fukasawa, "Motion and longitudinal strength of a ship in head sea and the effects of nonlinearlities," *Journal of the Society of Naval Architects of Japan*, Vol. 143 & 144, 1978, Vol. 145, 1979

[7] T.Kuroiwa, "A Study on Structural Response Acting on a Ship in Large Amplitude Waves," PhD. Thesis, Tokyo University, 1986

[8] Masataka Fujino, Bum Sang Yoon, "A Study on Wave Loads Acting on a Ship in Large Amplitude Waves (3rd Report)," *Journal of the Society of Naval Architects of Japan* , Vol. 158, 1985

[9] Jeom K. Paik, Chang Y. Kim, "Strength Analysis of Double Bottom Structures in Standing by Idealized Structural Unit Methods," *Trans. of The Society of Naval Architects of Korea*, Vol. 28.

[10] K. K. Shin, "A Study on the Dynamic Strength Analysis of the Hull Girder Among Waves," PhD Thesis of P.N.U., 1991

[11] Hisaaki Maeda, "Wave Excitation Forces on Two Dimensional Ships of Arbitary sections," *Journal of the Society of Naval Architects of Japan*, Vol. 126, 1969

[12] W. Frank, "Oscillation of Cylinder in or below free surface of deep fluid," NSRDC Report 2375, 1967

[13] J.W.Bedel and C.M.Lee, "Numerical calculation of the added mass and damping coefficients of cylinders oscillating in or below a free surface," NSRDC Report 3551, 1971

[14] C.Y. Kim, J. A. Kim, S. S. Kim, B. K. Hong, D. M. Bae, " A Study on the Response of the motions and Strength of Ships in waves taking account of Non-Linearities," *Trans. of the Society of Naval Architects of Korea*, Vol. 24. 1987

[15] ITTC, Report of Committee I.2, 10th ISSC, 1988

[16] Yusaku Kyozuka, "Non-Linear Hydrodynamic Forces Acting on Two- Dimensional Bodies (1st-4th Report)," *Journal of the Society of Naval Architects of Japan*, Vols. 148, 149, 150, 152 (1980-1983)

[17] Container Ship, J.S.R.A., 1968

[18] Korvin-Kroukovsky,B,V., "Investigation of Ship Motion in Regular Waves," *Trans. SNAME*, Vol. 63, 1953

[19] Salvesen,N.,Tuck,E.O., and Faltinsen,O., "Ship Motions and Sea Loads," *Trans. SNAME*, Vol. 78, 1970

[20] SNAME, Hydrodynamics in Ship Design, Vol. 3, 1965

[21] K.Ohtaka, et al,"On the Coupled Torsional - Horizontal Vibration of Ships," Mitsubishi Technical Bulletin, No. 54, 1967

[22] T.Kumai, "On the Coupled Torsional-Horizontal Vibration of Ships," *Journal of the Society of Naval Architects of Japan*, Vol. 100, 1957

[23] Y.Matsuura, et al, "Study on the coupled Torsional and Flexural Vibration of Ship with Large Hatch Openings(1st Report)," *The Society of Naval Architects of West Japan*, No. 127, 1968

[24] Y.Matsuura, et al, "Study on the coupled Torsional and Flexural Vibration of Ship with Large Hatch Openings(2nd Report)," *The Society of Naval Architects of West Japan*, No. 127, 1968

[25] G.A.Gunnlang and P.T.Perdersen, "A Finite Element Formulation for Beams with Thin Walled Cross-Sections," *Computer & Structure*, Vol. 15, No. 6, 1982

[26] Fukazawa T., Yamamoto Y., Fujino M., Motora S., "Motion and Longitudinal Strength of a Ship in Head Sea and the Effect of Non-linearities - Experiments," *Journal of the Society of Naval Architects of Japan*, Vol. 150 (1981), 308-314

[27] C.Y.Kim, D.S.Eom, S.S.Kim, J.K.Paik, "A Basic Study on the High Sophisticated Non-linear Structural Analysis and Rational Design of Ship Structure," Korea Science and Engineering Foundation, 89-0206-04, 1991

Table 1: Particulars of model

Length between Perpendiculars (L)	3.0000 m
Breadth Moulded (B)	0.4320 m
Depth Moulded (D)	0.2620 m
Draft at A.P (d_a)	0.1704 m
Draft at Midship (d_m)	0.1667 m
Draft at F.P (d_f)	0.1630 m
Displacement (Δ)	124.6000 kg
Block Coefficient (C_b)	0.5787
Center of Gravity from Midship (X_G)	0.0154 L
Longitudinal Gyradius (k_l)	0.2380 L
GM	0.0354 B

Table 2: Particulars of ship

Length between Perpendiculars (L)	180 m
Breadth Moulded (B)	32.2 m
Depth Moulded (D)	19.5 m
Draft at Full Load Condition	12 m
Draft at Half Load Condition	8.742 m
Displacement at Half Load Condition	35468 m^2
GM	3.4 m

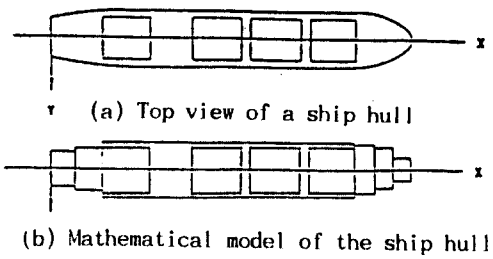

Figure 1 : Example for the simplification of a ship hull

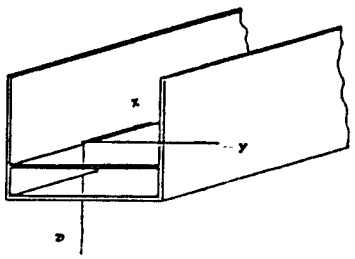

Figure 2 : Beam with thin walled cross-section

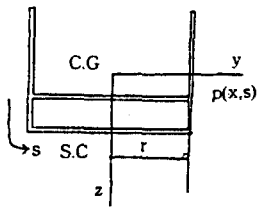

Figure 3 : Coordinate system

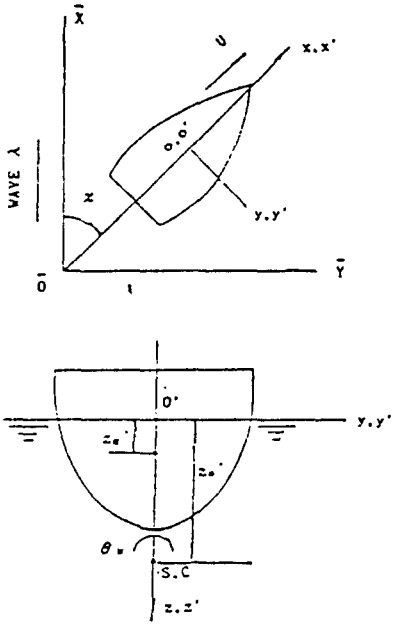

Figure 4 : Coordinate system for wave load

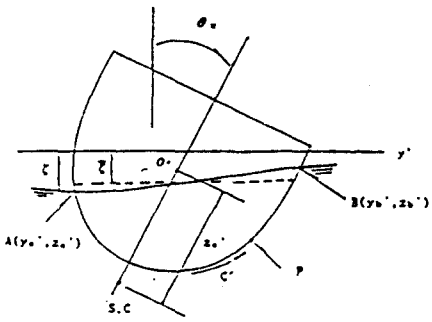

Figure 5 : Ship section configuration

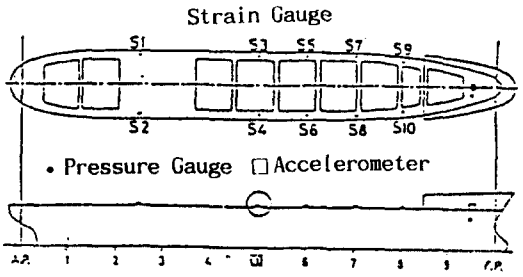

Figure 6 : Locations of gauges(ref.[26])

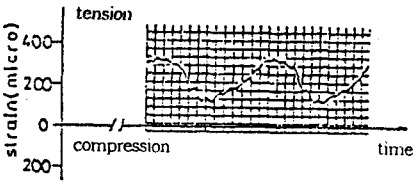

(a) Experiment(ref. [26]

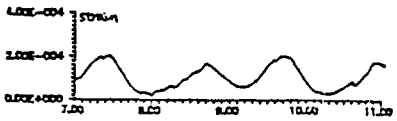

(b) Calculation

Figure 7 : Time history of check strain at midship ($F_n = 154, x = 157.5°, \lambda/L = 1.2, L/H_w = 30$)

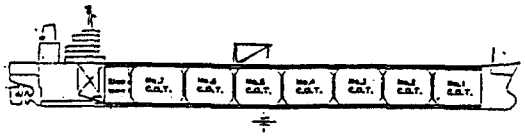

Figure 8 : Profile of double skin tanker

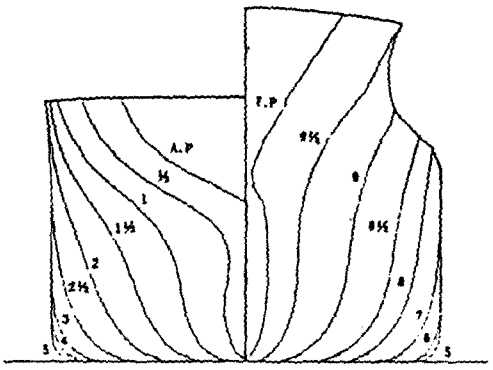

Figure 9 : Body plan of double skin tanker

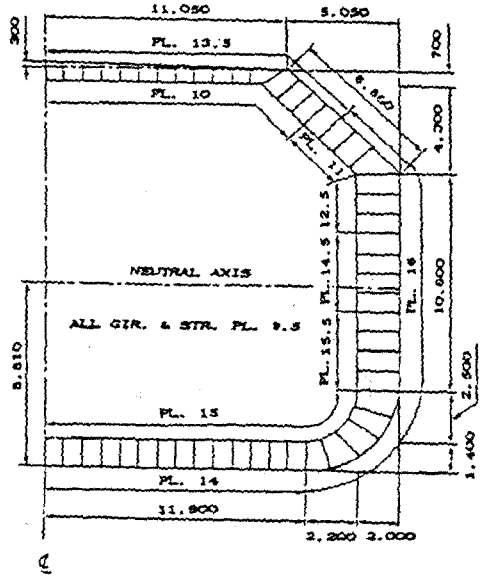

Figure 10 : Midship section of double skin tanker

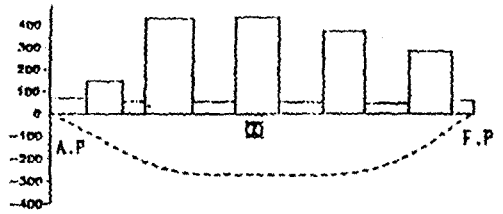

(a) Weighted and buoyance distribution of ship

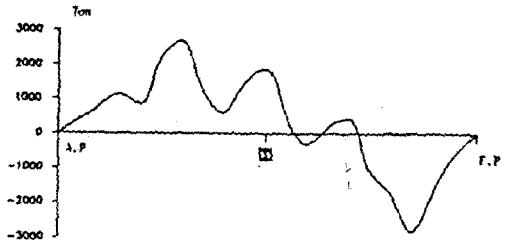

(b) Shear force diagram of ship

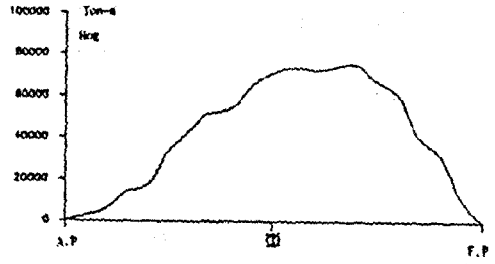

(c) Bending moment diagram of ship

Figure 11 : Still water condition of ship

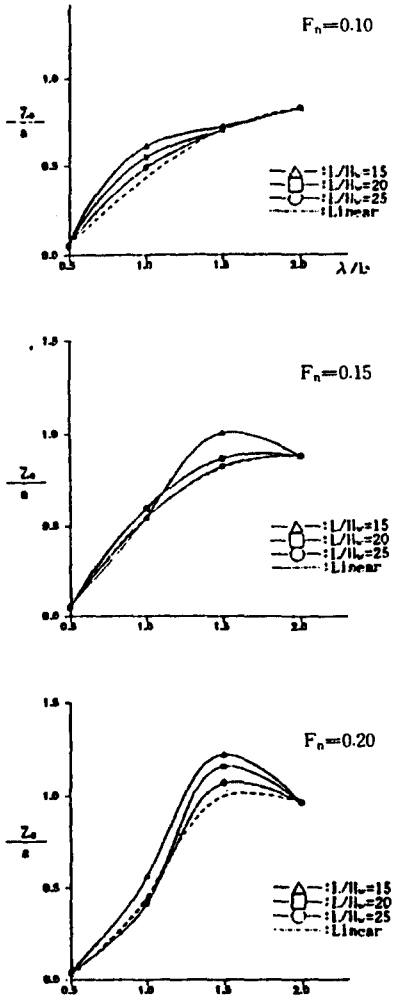

Figure 12: Heave response of ship in head wave

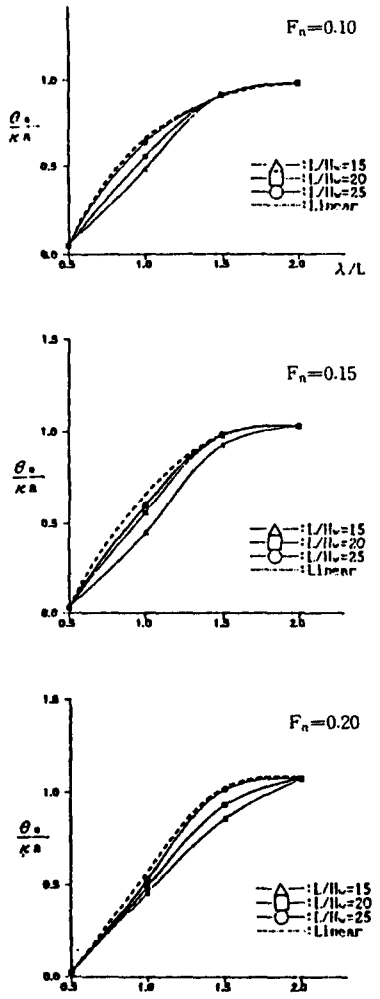

Figure 13 : Pitch response of ship in head wave

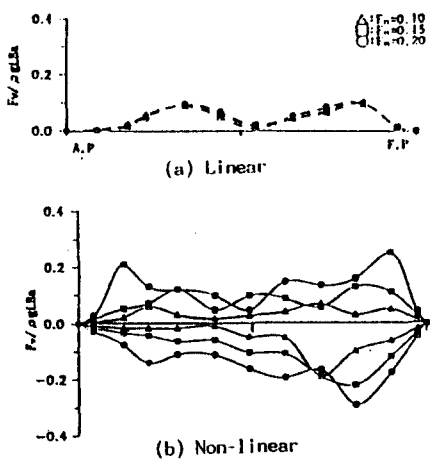

Figure 14 : Distribution of vertical shear force in head wave($\lambda/L = 1.0$)

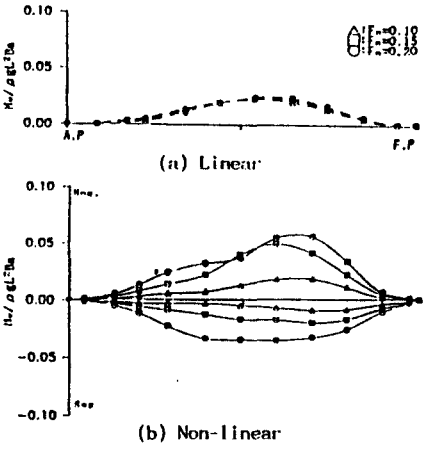

Figure 15 : Distribution of vertical bending moment in head wave($\lambda/L = 1.0$)

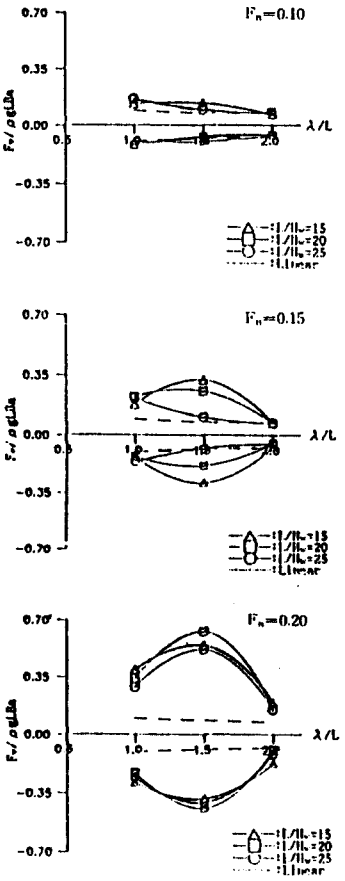

Figure 16 : Maximum vertical shear force in head wave

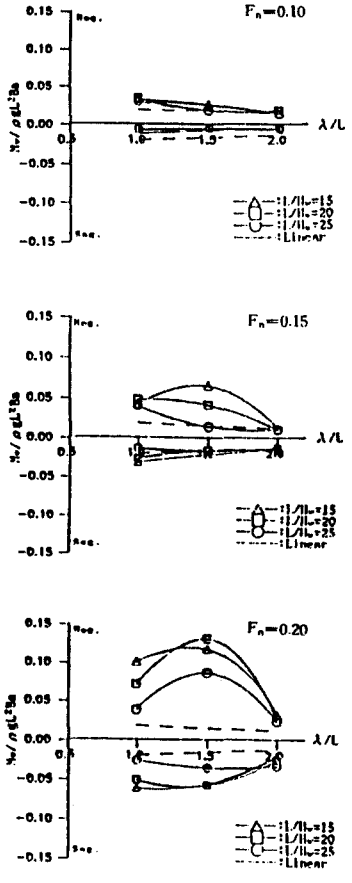

Figure 17 : Maximum vertical bending moment in head wave

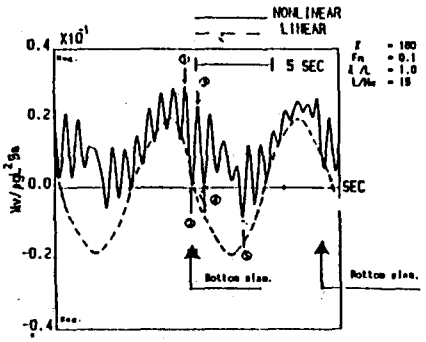

(a) Time history of vertical bending moment in head wave

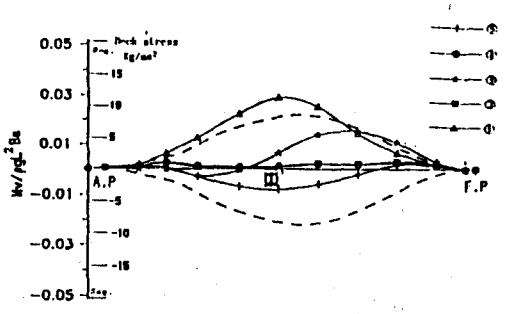

(b) Distribution of vertical bending moment in head wave

Figure 18 : Vertical bending moment in head wave when F_n=0.1

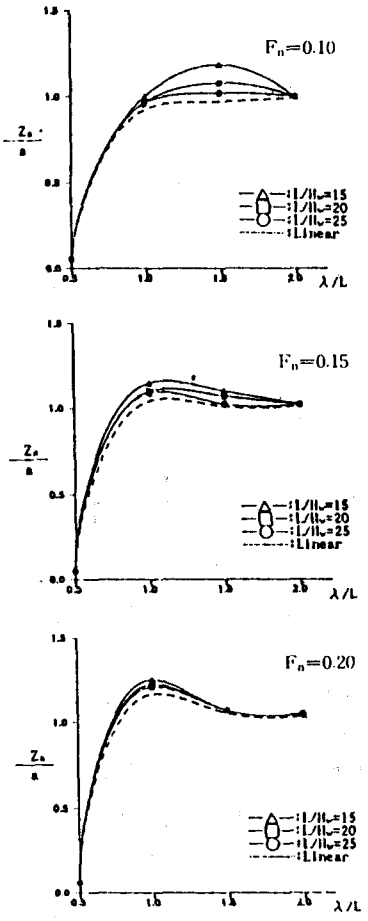

Figure 19 : Heave response of ship in oblique wave

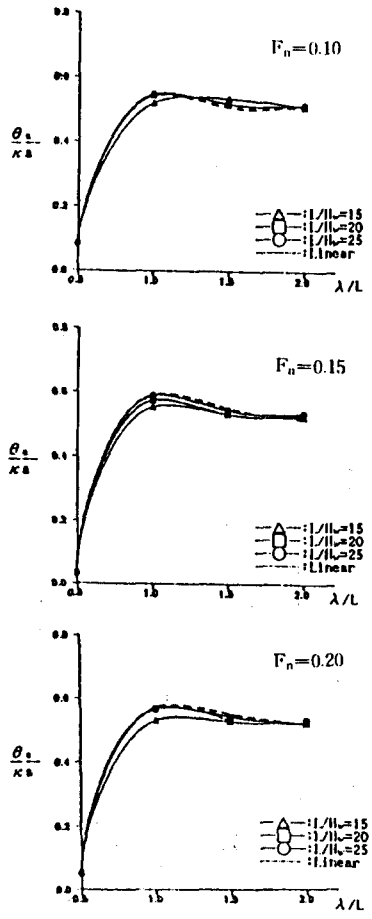

Figure 20 : Pitch response of ship in oblique wave

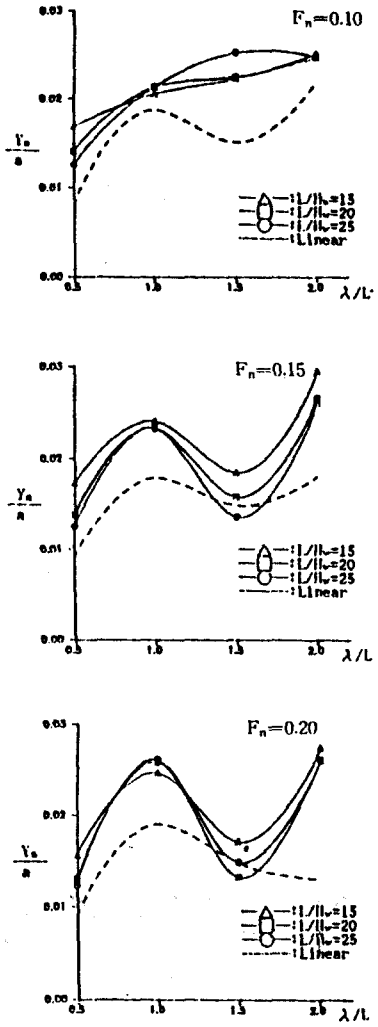

Figure 21 : Sway response of ship in oblique wave

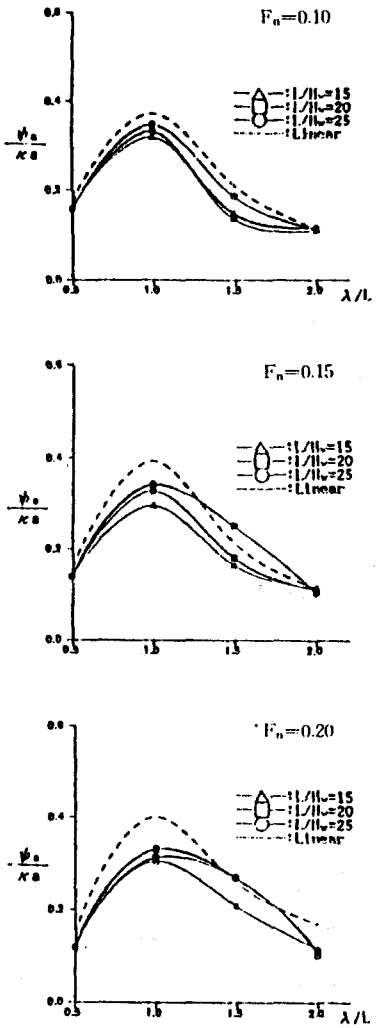

Figure 22 : Yaw response of ship in oblique wave

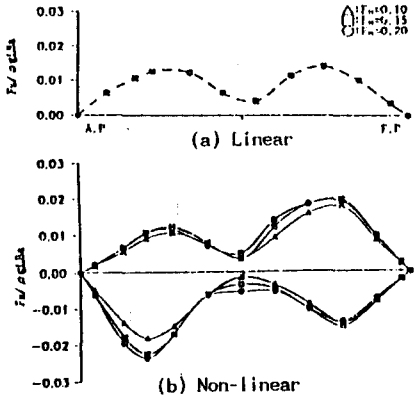

Figure 25 : Distribution of vertical bending moment oblique wave($\lambda/L = 1.0$)

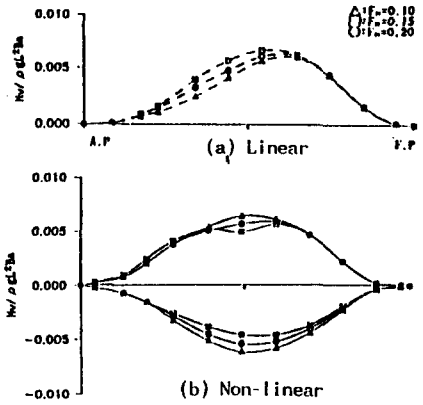

Figure 26 : Distribution of horizontal shear force in oblique wave($\lambda/L = 1.0$)

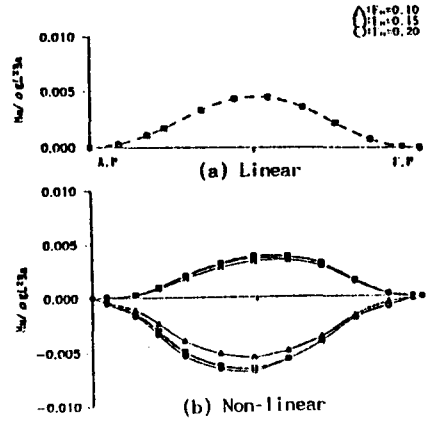

Figure 27 : Distribution of horizontal bending moment in oblique wave($\lambda/L = 1.0$)

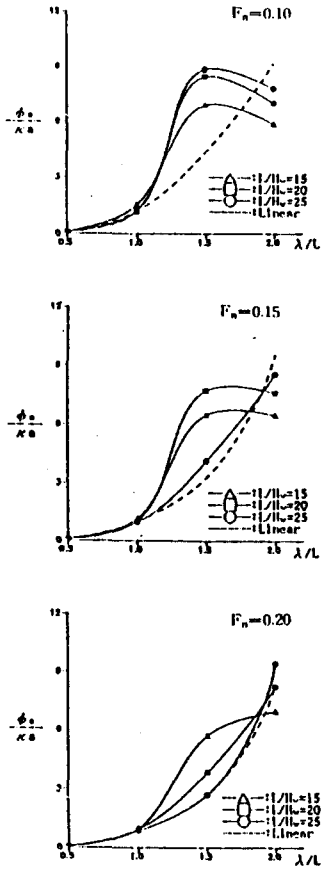

Figure 23 : Roll response of ship in oblique wave

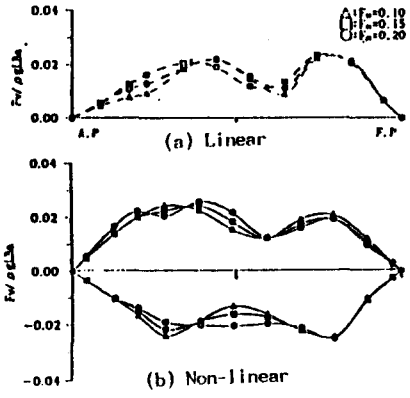

Figure 24 : Distribution of vertical shear force in oblique wave($\lambda/L = 1.0$)

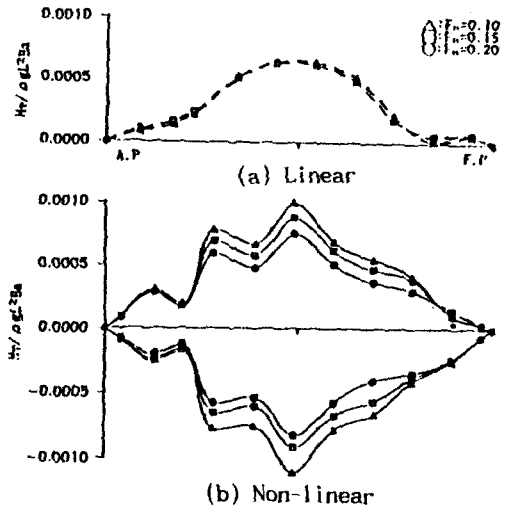

Figure 28 : Distribution of torsional moment in oblique wave($\lambda/L = 1.0$)

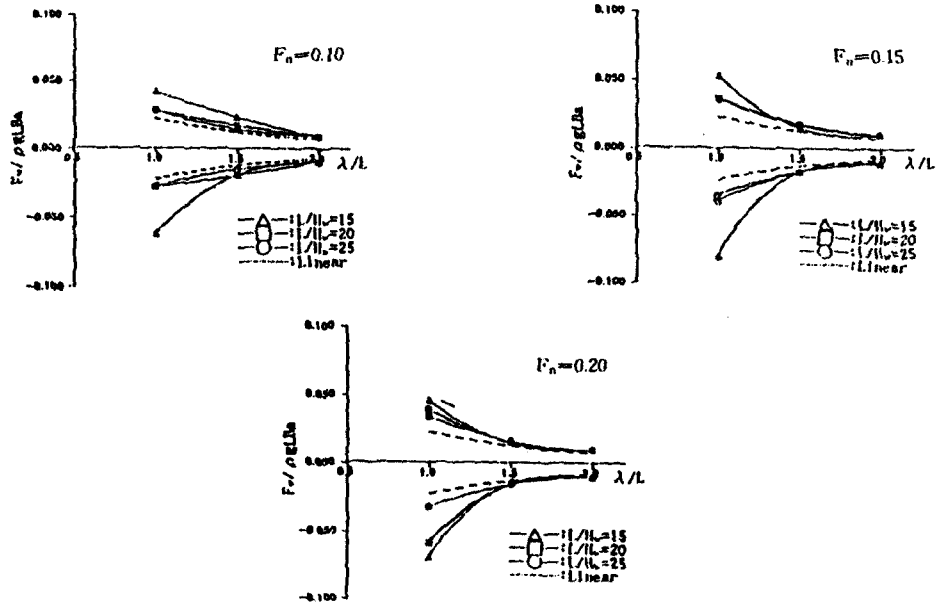

Figure 29 : Maximum vertical shear force in oblique wave

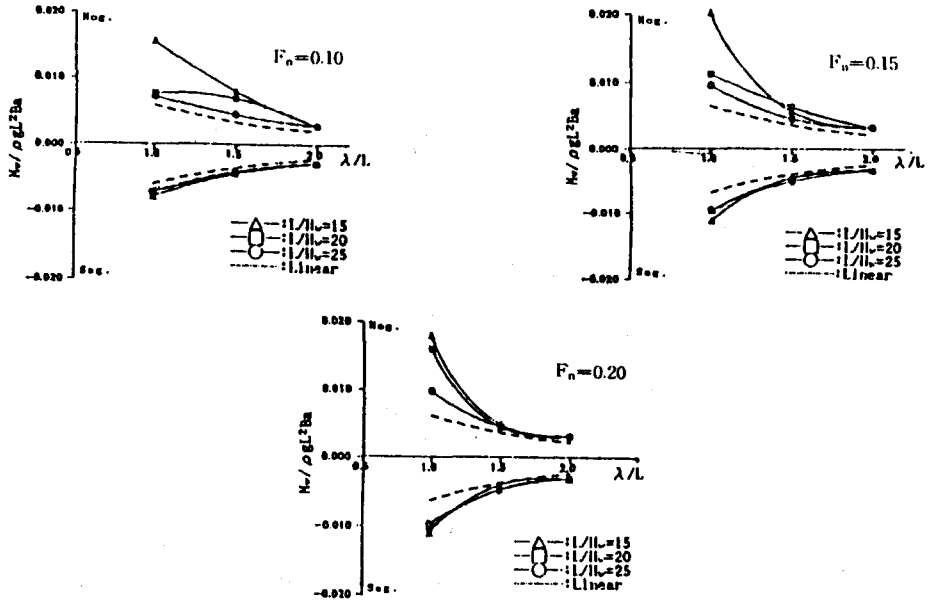

Figure 30 : Maximum vertical bending moment in oblique wave

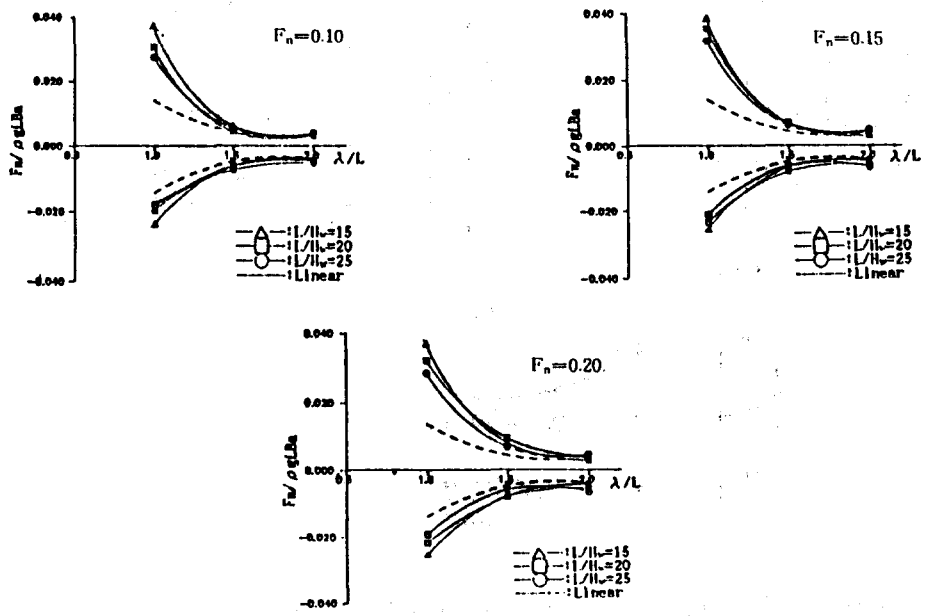

Figure 31 : Maximum horizontal shear force in oblique wave

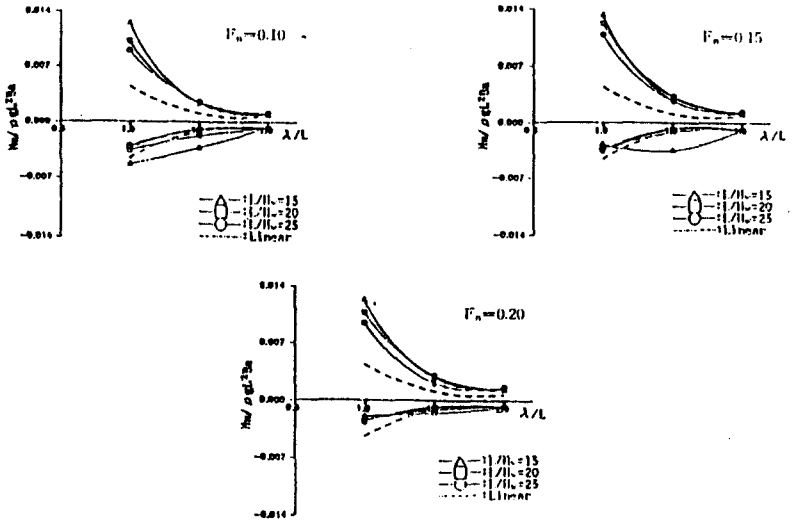

Figure 32 : Maximum horizontal bending moment in oblique wave

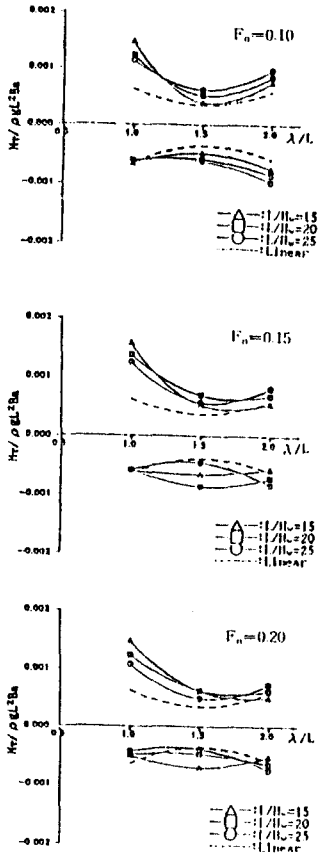

Figure 33 : Maximum torsional moment in oblique wave